11-29-2005

Dynamics of a Nanomechanical Resonator Coupled to a Superconducting Single-Electron Transistor

M. P. Blencowe
Dartmouth College

J. Imbers
University of Nottingham

A. D. Armour
University of Nottingham

Dynamics of a nanomechanical resonator coupled to a superconducting single-electron transistor

New Journal of Physics
The open–access journal for physics

Dynamics of a nanomechanical resonator coupled to a superconducting single-electron transistor

M P Blencowe[1], J Imbers[2] and A D Armour[2,3]

[1] Department of Physics and Astronomy, 6127 Wilder Laboratory, Dartmouth College, Hanover, NH 03755, USA
[2] School of Physics and Astronomy, University of Nottingham, Nottingham NG7 2RD, UK
E-mail: miles.p.blencowe@dartmouth.edu, ppxji@nottingham.ac.uk and andrew.armour@nottingham.ac.uk

New Journal of Physics **7** (2005) 236
Received 27 July 2005
Published 29 November 2005
Online at http://www.njp.org/
doi:10.1088/1367-2630/7/1/236

Abstract. We present an analysis of the dynamics of a nanomechanical resonator coupled to a superconducting single-electron transistor (SSET) in the vicinity of Josephson quasi-particle (JQP) and double Josephson quasi-particle (DJQP) resonances. For weak coupling and wide separation of dynamical timescales, we find that for either superconducting resonances the dynamics of the resonator are given by a Fokker–Planck equation, i.e. the SSET behaves effectively as an equilibrium heat bath, characterized by an effective temperature, which also damps the resonator and renormalizes its frequency. Depending on the gate and drain–source voltage bias points with respect to the superconducting resonance, the SSET can also give rise to an instability in the mechanical resonator marked by negative damping and temperature within the appropriate Fokker–Planck equation. Furthermore, sufficiently close to a resonance, we find that the Fokker–Planck description breaks down. We also point out that there is a close analogy between coupling of a nanomechanical resonator to an SSET in the vicinity of the JQP resonance and Doppler cooling of atoms by means of lasers.

[3] Author to whom any correspondence should be addressed.

PII: S1367-2630(05)04459-9

Contents

1. Introduction

Nanomechanical single-electron transistors (SETs), in which a mechanical resonator forms the voltage gate of the transistor, constitute a new and interesting class of nanoelectromechanical system. The idea of coupling a nanomechanical resonator to the island of an SET as a mechanically compliant voltage gate was proposed as a way of measuring the displacement of a mechanical resonator with high precision [1]–[4], since the conductance properties of the SET are extremely sensitive to the resonator motion. Indeed such devices have recently been used to measure the displacement of a nanomechanical resonator with almost quantum-limited precision [5, 6].

The sensitivity with which an SET can be used to measure the position of a nanomechanical resonator is ultimately limited by the back-action of the SET on the dynamics of the resonator. The back-action of electrons moving through a normal state SET gated by a nanomechanical resonator was studied recently [7]–[10] and it was shown that, in the regime where the energy associated with the applied bias voltage is much larger than the resonator energy quanta, the SET electrons act on the nanomechanical resonator in a way which is closely analogous to an equilibrium thermal bath. In fact, the dynamics of the resonator can be described by a Fokker–Planck equation for a damped harmonic oscillator in contact with a thermal bath at a fixed temperature [10]. Very similar results were obtained explicitly for a resonator coupled to a tunnel junction [11, 12] and it was also shown by Clerk [13] that such behaviour is expected to be generic within the regime of linear response.

In contrast to normal state SETs, where the current arises solely from electron tunnelling and cotunnelling processes [14], superconducting SETs (SSETs) can support a wide range of different electronic processes which contribute to the current including tunnelling or cotunnelling of quasi-particles, coherent tunnelling of Cooper pairs and even Andreev reflection [15]–[20]. Furthermore, there exist a number of current resonances for particular values of the drain–source and gate voltages of the SSET, where current is carried by a combination of different processes occurring at the source and drain junctions in turn. The best known (and most readily observed experimentally) current resonances for the SSET are the Josephson quasi-particle (JQP) and double Josephson quasi-particle (DJQP) cycles, where transport occurs via a combination

of coherent, resonant tunnelling of Cooper pairs and incoherent quasi-particle tunnelling [15]–[20].

In this paper, we analyse the back-action of an SSET on a nanomechanical resonator. In particular, we investigate the dynamics of a resonator coupled as a voltage-gate to an SSET, which is tuned in the vicinity of the JQP or the DJQP resonance. We find that for both resonances, the resonator can act as though it were coupled to a thermal bath with its dynamics described by a Fokker–Planck equation, as was found for the normal state SET. However, the magnitudes of the effective temperature and damping of the resonator in the vicinity of the JQP and DJQP resonances differ substantially, both from each other and from those for the normal state case. A resonator coupled to a normal state SET has an effective temperature, which is proportional to the drain–source voltage applied to the SET and is always damped. In contrast, the effective temperature of a resonator coupled to an SSET in the vicinity of JQP or DJQP resonance is largely controlled by how far the SSET is biased from the resonance, rather than the magnitude of the drain–source voltage, and hence can easily be an order of magnitude smaller than the effective temperature for an analogous normal state SET. Furthermore, as the applied gate and drain–source voltages are adjusted to tune the SSET through a given JQP resonance, we find that the Fokker–Planck description breaks down sufficiently close to the resonance; while further from the resonance on the other side, the Fokker–Planck description is restored once again, but with negative effective temperature and resonator damping constant, implying the possibility of a dynamic instability. Very similar results for the SSET-resonator system have also been obtained independently using a different approach by Clerk and Bennett [21].

The dynamics of a nanomechanical resonator coupled to an SSET in the vicinity of the JQP resonance bears a striking resemblance to a number of other physical systems. In particular, the behaviour of the effective temperature of the resonator in the vicinity of the JQP resonance takes a very similar form to that of atoms undergoing Doppler cooling due to their interactions with laser light [22, 23]. Indeed, the minimum effective temperature of both a resonator in the vicinity of the JQP resonance and Doppler-cooled atoms are given by a decay rate: the quasi-particle decay rate for the SSET-resonator system and the decay rate of the excited state for the atoms.

This paper is organized as follows. In section 2, we introduce a master equation describing the coupled statistical dynamics of the SSET-resonator system in the vicinity of the JQP resonance (a similar master equation for the SSET-resonator system in the vicinity of the DJQP resonance is described in the appendix). We then show that the master equation can be well approximated by a Fokker–Planck equation under conditions of weak coupling and wide separation of SSET and oscillator dynamics timescales. In section 3, we present analytic and numerical calculations of the SSET-induced damping, frequency renormalization and effective temperature in the vicinity of the JQP and DJQP resonances. In section 4, we discuss our results and the analogy between the SSET-resonator device and other physical systems, before we finally present our conclusions.

2. Master equation description for the JQP resonance

In this section, we obtain a master equation for the SSET-resonator system in the vicinity of the JQP resonance and show that the dynamics of the resonator can be described by a Fokker–Planck equation. The same approach can also be used to derive analogous results for the DJQP resonance, details of which are given in the appendix.

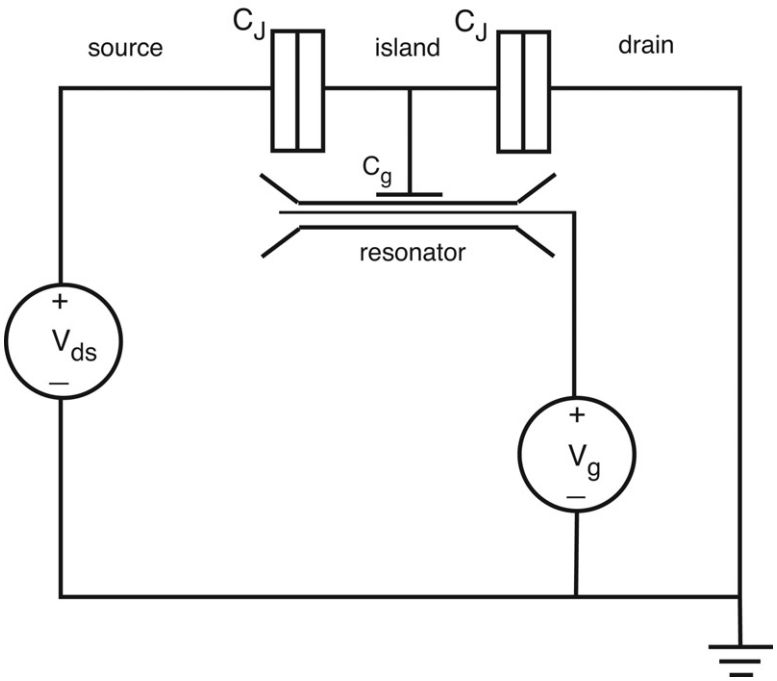

Figure 1. Model circuit of the SSET-resonator system.

The model circuit that we consider is shown in figure 1. The SSET consists of a small superconducting island and two superconducting leads, weakly linked to the island via tunnel junctions with capacitances C_J; a drain–source bias voltage V_{ds} is applied to the leads. The nanomechanical resonator is treated as a single-mode harmonic oscillator with frequency ω and mass m. The metallized resonator is located adjacent the SSET island, forming a gate with capacitance $C_g(x)$, which depends on the resonator's displacement x; a gate voltage V_g is applied to the resonator. In the experiments of [5, 6], the coupling between the SSET island and the resonator is typically very weak so that the displacement of the resonator from its equilibrium position is much less than the separation d between that equilibrium position and the SSET island itself. Hence, if we also assume a parallel-plate geometry for simplicity, the gate capacitance can be approximated by [8]: $C_g(x) = C_g(1 - x/d)$, implying linear coupling between the SSET and the resonator [13].

The central island of the SSET is taken to be sufficiently small that its charging energy $E_c = e^2/2(2C_J + C_g) \sim \Delta \gg k_B T$, where Δ is the superconducting gap and T the temperature of the quasi-particles in the leads. Hence, the number of charge states accessible to the island is severely restricted. The Josephson coupling between the leads and the island is $E_J = h\Delta/(8e^2 R_J) \ll E_c$, where R_J is the resistance of the junctions [19]. Depending on the exact value of the polarization charge induced on the SSET island by the resonator gate, $N_g = (C_g V_g + C_J V_{ds})/e$, certain quasi-particle and resonant Cooper-pair tunnelling processes can become energetically favourable leading to a number of possible current-carrying regimes such as the JQP and DJQP cycles. At sufficiently large drain–source voltages, and for relatively low-junction resistances, it is also possible for current to flow via higher-order processes such as quasi-particle cotunnelling, but we will neglect such effects in what follows.

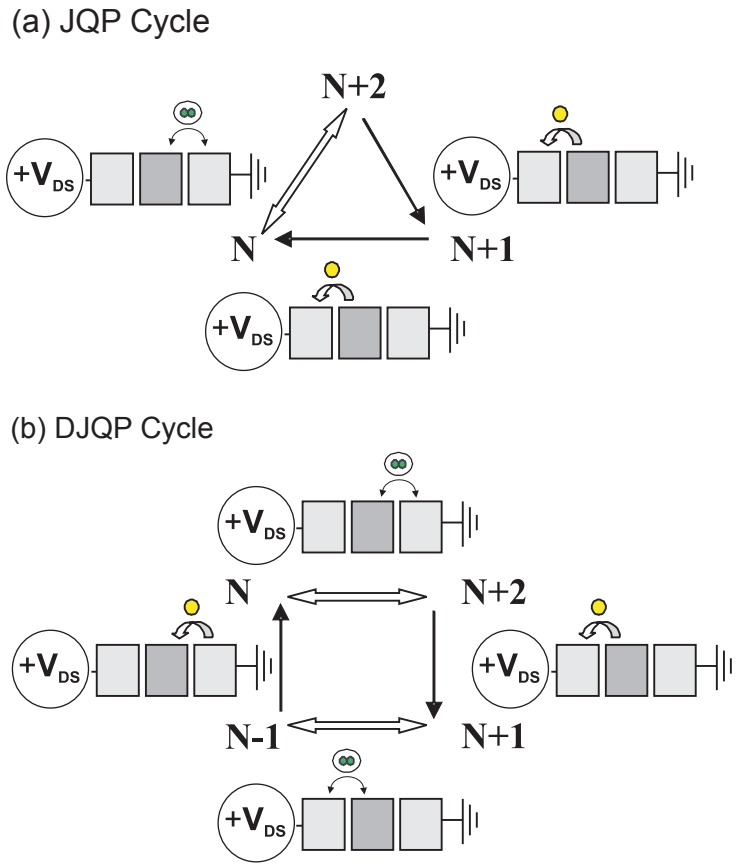

Figure 2. Schematic illustration of the JQP and DJQP cycles. (a) For the JQP cycle, Josephson tunnelling involving a Cooper pair occurs between drain and island electrodes, increasing the island electron number N by 2, followed by two, subsequent quasi-particle tunnel decay processes into the source electrode, decreasing the electron island number by 2 [18]. (b) For the DJQP cycle, Josephson tunnelling of a Cooper pair occurs at both junctions, with a Cooper-pair tunnelling event through a given junction alternating in turn with a quasi-particle tunnelling event at the opposite junction [19].

The details of the specific electronic processes which occur at the JQP and DJQP resonances are illustrated schematically in figure 2. Close to the JQP resonance, Cooper pairs tunnel between the right (with reference to the circuit in figure 1), drain electrode and island, while electron quasi-particles tunnel out from the island to the left source electrode. Alternatively, Cooper-pair tunnelling can occur between the left source electrode and island, while electron quasi-particles tunnel in from the right-drain electrode to the island. Which of these two JQP cycles take place depends on the gate and drain–source voltage biases. We shall consider biases such that only the former cycle occurs (i.e. that illustrated in figure 2(a)).

We seek a master equation that describes the dynamics of the island charge state of the SSET and the position–velocity state of the resonator's centre-of-mass valid in the vicinity of the JQP resonance. Master equations for the island charges in normal state and SSETs have

been derived by a number of groups using essentially the same technique [14, 18]. Starting with the full (time-dependent) Schrödinger equation for the system, one can trace over the microscopic electronic degrees of freedom making use of a second-order Born approximation (that treats the quasi-particle tunnelling rates between the island and the leads as a small expansion parameter), followed by a long-time limit Markov approximation (that treats the response of the electrons in the leads to a tunnelling event as being instantaneous), to arrive at a master equation for a reduced density matrix represented in the basis of total number of electrons, N, on the island. We generalize this approach to include the resonator. Again starting from a fully quantum Hamiltonian, we follow the same procedure of the Born and Markov approximations and trace over the microscopic degrees of freedom. However, we also assume that the resonator does not evolve at all on the timescale of the quasi-particle tunnelling processes. Essentially this means that we are treating the resonator as a classical oscillator.[4] Finally, we take the Wigner transform [24] of the resulting equations to obtain the desired master equation, which can be thought of as providing a semiclassical description of the coupled dynamics [25].

For the JQP process (see figure 2(a)), the island electron number can be N, $N+1$ or $N+2$, with the N and $N+2$ number states linked by coherent Cooper-pair tunnelling. Hence, the associated set of coupled semiclassical master equations has diagonal components $\rho_N(x, v, t)$, $\rho_{N+1}(x, v, t)$ and $\rho_{N+2}(x, v, t)$, and off-diagonal component $\rho_{N,N+2}(x, v, t) = \rho^*_{N+2,N}(x, v, t)$, where x and v are the position and velocity coordinates, respectively, of the oscillator. In our semiclassical description, the sum $\rho_N(x, v, t) + \rho_{N+1}(x, v, t) + \rho_{N+2}(x, v, t)$ is the probability density $P_{\mathrm{HO}}(x, v, t)$ of finding the oscillator at the point in phase space (x, v) at time t, while the integral $\int \mathrm{d}x\, \mathrm{d}v\, \rho_N(x, v, t)$ gives the probability $P_N(t)$ that the island electron number is N at time t, with the probability conservation $P_N + P_{N+1} + P_{N+2} = 1$. Explicitly, the semiclassical master equations take the form

$$\dot{\rho}_N = \omega^2(x + Nx_s)\frac{\partial \rho_N}{\partial v} - v\frac{\partial \rho_N}{\partial x} + \mathrm{i}\frac{E_J}{2\hbar}(\rho_{N+2,N} - \rho_{N,N+2}) + [\Gamma(E_{N+1,N}) + \Gamma'(E_{N+1,N})m\omega^2 x_s x]\,\rho_{N+1},$$

$$\dot{\rho}_{N+2} = \omega^2[x + (N+2)x_s]\frac{\partial \rho_{N+2}}{\partial v} - v\frac{\partial \rho_{N+2}}{\partial x} - \mathrm{i}\frac{E_J}{2\hbar}(\rho_{N+2,N} - \rho_{N,N+2}) - [\Gamma(E_{N+2,N+1}) + \Gamma'(E_{N+2,N+1})m\omega^2 x_s x]\,\rho_{N+2},$$

$$\dot{\rho}_{N+1} = \omega^2[x + (N+1)x_s]\frac{\partial \rho_{N+1}}{\partial v} - v\frac{\partial \rho_{N+1}}{\partial x} + [\Gamma(E_{N+2,N+1}) + \Gamma'(E_{N+2,N+1})m\omega^2 x_s x]\,\rho_{N+2} - [\Gamma(E_{N+1,N}) + \Gamma'(E_{N+1,N})m\omega^2 x_s x]\,\rho_{N+1},$$

[4] In deriving the quasi-particle tunnelling terms, we effectively treat the resonator as a classical oscillator by making an adiabatic approximation, i.e. we assume that it does not move on the timescale of the tunnelling processes, an approximation which was also used in [8]. The other terms in the master equations which arise from the coherent evolution of the resonator and SSET charges are not affected by the adiabatic approximation. As we shall see later on, the position dependence of the quasi-particle transition rates in fact do not play an important role in affecting the resonator dynamics near the JQP resonance, so we expect our master equations to provide a description of the resonator dynamics close to the JQP resonance, which is essentially the same as that which would be obtained from a fully quantum derivation.

$$\dot{\rho}_{N,N+2} = \omega^2[x + (N+1)x_s]\frac{\partial \rho_{N,N+2}}{\partial v} - v\frac{\partial \rho_{N,N+2}}{\partial x} + \mathrm{i}\frac{E_J}{2\hbar}(\rho_{N+2} - \rho_N)$$
$$+ \frac{\mathrm{i}}{\hbar}(E_{N+2,N} + 2m\omega^2 x_s x)\rho_{N,N+2} - \tfrac{1}{2}[\Gamma(E_{N+2,N+1}) + \Gamma'(E_{N+2,N+1})m\omega^2 x_s x]\,\rho_{N,N+2}, \tag{1}$$

where $x_s = 2E_c C_g V_g/(em\omega^2 d)$, which is the distance between equilibrium positions of the oscillator with N and $N+1$ electrons on the island, parametrizing the strength of the electro-mechanical coupling. The quasi-particle tunnel rates are given by [26]

$$\Gamma(E) = \frac{1}{e^2 R_J}\int_{-\infty}^{\infty} \mathrm{d}\epsilon\, \rho(\epsilon)\rho(\epsilon + E)n(\epsilon)[1 - n(\epsilon + E)], \tag{2}$$

where

$$\rho(\epsilon) = \sqrt{\frac{\epsilon^2}{\epsilon^2 - \Delta^2}}\,\Theta(\epsilon^2 - \Delta^2) \tag{3}$$

is the normalized quasi-particle density of states, with $\Theta(\cdot)$ the stepfunction, and $n(\epsilon) = 1/(1 + \exp(\epsilon/k_B T))$. In the above master equations, the typical position coordinate is assumed sufficiently small that the tunnel rates can be expanded to first order in the position coordinate, with $\Gamma'(E) = \mathrm{d}\Gamma/\mathrm{d}E$. The quantities $E_{N+2,N+1}$ and $E_{N+1,N}$ are the energies gained by an electron, when it tunnels from island to source electrode, the island number changing from $N+2$ to $N+1$ and $N+1$ to N, respectively. The quantity $E_{N+2,N}$ is the energy gained by a Cooper pair, when it tunnels from island to drain electrode. These energies are as follows:

$$\begin{aligned} E_{N+2,N+1} &= -2E_c(N_g - N - 3/2) + eV_{ds}, \\ E_{N+1,N} &= -2E_c(N_g - N - 1/2) + eV_{ds}, \\ E_{N+2,N} &= -4E_c(N_g - N - 1). \end{aligned} \tag{4}$$

The JQP resonance condition is $E_{N+2,N} = 0$, which is satisfied for $N_g = N + 1$. Furthermore, the bias voltage must be sufficiently large for the quasi-particle processes to be allowed, enabling the JQP cycle. For superconductors at zero temperature, this translates into the requirement that $eV_{ds} > 2\Delta + E_c$. Notice also that in the absence of the mechanical oscillator, we recover the standard master equations for the SSET about the JQP resonance [18].

It is convenient to express the master equation in terms of dimensionless coordinates, since in dimensionless form the essential parameters governing the dynamics are more clearly expressed. Rewriting the time coordinate in units of the tunnelling time, $\tau_{\mathrm{tunnel}} = eR_J/V_{ds}$, the position coordinate in units of x_s, and the velocity coordinate in units of $x_s/\tau_{\mathrm{tunnel}}$, the master equations take the form

$$\dot{\rho}_N = \epsilon_{\mathrm{HO}}^2(x + N)\frac{\partial \rho_N}{\partial v} - v\frac{\partial \rho_N}{\partial x} + \mathrm{i}\pi\epsilon_J(\rho_{N+2,N} - \rho_{N,N+2}) + [\tilde{\Gamma}(\tilde{E}_{N+1,N}) + \tilde{\Gamma}'(\tilde{E}_{N+1,N})\kappa x]\,\rho_{N+1},$$

$$\dot{\rho}_{N+2} = \epsilon_{\mathrm{HO}}^2[x + (N+2)]\frac{\partial \rho_{N+2}}{\partial v} - v\frac{\partial \rho_{N+2}}{\partial x} - \mathrm{i}\pi\epsilon_J(\rho_{N+2,N} - \rho_{N,N+2})$$
$$- [\tilde{\Gamma}(\tilde{E}_{N+2,N+1}) + \tilde{\Gamma}'(\tilde{E}_{N+2,N+1})\kappa x]\,\rho_{N+2},$$

$$\dot{\rho}_{N+1} = \epsilon_{\mathrm{HO}}^2[x + (N+1)]\frac{\partial \rho_{N+1}}{\partial v} - v\frac{\partial \rho_{N+1}}{\partial x} + [\tilde{\Gamma}(\tilde{E}_{N+2,N+1}) + \tilde{\Gamma}'(\tilde{E}_{N+2,N+1})\kappa x]\,\rho_{N+2}$$
$$- [\tilde{\Gamma}(\tilde{E}_{N+1,N}) + \tilde{\Gamma}'(\tilde{E}_{N+1,N})\kappa x]\,\rho_{N+1},$$
$$\dot{\rho}_{N,N+2} = \epsilon_{\mathrm{HO}}^2[x + (N+1)]\frac{\partial \rho_{N,N+2}}{\partial v} - v\frac{\partial \rho_{N,N+2}}{\partial x} + \mathrm{i}\pi\epsilon_J(\rho_{N+2} - \rho_N)$$
$$+ 2\pi \mathrm{i} r(\tilde{E}_{N+2,N} + 2\kappa x)\rho_{N,N+2} - \tfrac{1}{2}[\tilde{\Gamma}(\tilde{E}_{N+2,N+1}) + \tilde{\Gamma}'(\tilde{E}_{N+2,N+1})\kappa x]\,\rho_{N,N+2}. \quad (5)$$

The definitions of the various dimensionless parameters are as follows: $\epsilon_{\mathrm{HO}} = \omega\tau_{\mathrm{tunnel}}$ is the ratio of the SET quasi-particle tunnelling time to the oscillator period, $\epsilon_J = \tau_{\mathrm{tunnel}}/\tau_{\mathrm{Rabi}} = (eR_J/V_{ds})(E_J/h) = \Delta/(8eV_{ds})$ is the ratio of the quasi-particle tunnelling time to the Cooper-pair Rabi oscillation period, $r = R_J/(h/e^2)$ is the ratio of the tunnel junction resistance to the quantum of resistance, and $\kappa = m\omega^2 x_s^2/(eV_{ds})$ characterizes the coupling strength between the oscillator and the SET. The dimensionless tunnelling rate is

$$\tilde{\Gamma}(\tilde{E}) = \int_{-\infty}^{\infty} \mathrm{d}\tilde{\epsilon}\,\rho(\tilde{\epsilon})\rho(\tilde{\epsilon} + \tilde{E})n(\tilde{\epsilon})[1 - n(\tilde{\epsilon} + \tilde{E})], \quad (6)$$

where now

$$\rho(\tilde{\epsilon}) = \sqrt{\frac{\tilde{\epsilon}^2}{\tilde{\epsilon}^2 - \tilde{\Delta}^2}}\,\Theta(\tilde{\epsilon}^2 - \tilde{\Delta}^2) \quad (7)$$

and $n(\tilde{\epsilon}) = 1/(1 + \exp(\tilde{\epsilon}eV_{ds}/k_{\mathrm{B}}T))$, with $\tilde{\epsilon} = \epsilon/(eV_{ds})$, $\tilde{E} = E/(eV_{ds})$ and $\tilde{\Delta} = \Delta/(eV_{ds})$. Note that for typical nanomechanical SSETs [5, 6], we have $\epsilon_{\mathrm{HO}} \ll \epsilon_J \ll 1$, $\kappa \ll 1$ and $r \geqslant 1$. Also, the dimensionless quasi-particle tunnel rates $\tilde{\Gamma}$, and their gradients $\tilde{\Gamma}'$, are generally of order unity.

Our goal is to obtain a description of the dynamics of the resonator, decoupled from the details of the electronic degrees of freedom. One very direct way to obtain the resonator dynamics is to solve numerically the above master equation for the oscillator probability density $P_{\mathrm{HO}}(x, v, t)$. Another direction is to take advantage of the typical conditions of weak coupling ($\kappa \ll 1$) and wide separation of timescales ($\epsilon_{\mathrm{HO}} \ll 1$) to derive from the above master equation a much simpler, approximate effective equation for the oscillator probability density $P_{\mathrm{HO}}(x, v, t)$ (i.e. a reduced master equation for the oscillator alone) which can then be easily solved. We have used both approaches. In the remainder of this section, we describe how the reduced master equation is obtained and show that it is nothing other than the Fokker–Planck equation. Later in section 3, we compare the results of this approach with direct numerical integrations of the original set of master equations.

We begin our derivation of the reduced master equation of the resonator by rewriting the full set of the master equations (5) in the following, concise 5×5 matrix operator form:

$$\dot{\mathcal{P}} = (\mathcal{H}_0 + \mathcal{V})\mathcal{P}, \quad (8)$$

where

$$\mathcal{P} = \begin{pmatrix} \rho_{N+2}(x,v,t) \\ \rho_{N}(x,v,t) \\ \rho_{N+1}(x,v,t) \\ \mathrm{Im}\rho_{N,N+2}(x,v,t) \\ \mathrm{Re}\rho_{N,N+2}(x,v,t) \end{pmatrix},$$

$$\mathcal{H}_0 = \left(\epsilon_{\mathrm{HO}}^2 x\tfrac{\partial}{\partial v} - v\tfrac{\partial}{\partial x}\right)\mathcal{I} + \begin{pmatrix} -\Gamma_{N+2,N+1} & 0 & 0 & -2\pi\epsilon_J & 0 \\ 0 & 0 & \Gamma_{N+1,N} & 2\pi\epsilon_J & 0 \\ \Gamma_{N+2,N+1} & 0 & -\Gamma_{N+1,N} & 0 & 0 \\ \pi\epsilon_J & -\pi\epsilon_J & 0 & -\dfrac{\Gamma_{N+2,N+1}}{2} & 2\pi r E_{N+2,N} \\ 0 & 0 & 0 & -2\pi r E_{N+2,N} & -\dfrac{\Gamma_{N+2,N+1}}{2} \end{pmatrix}, \tag{9}$$

with $\mathcal{I}$ denoting the 5×5 identity matrix and we use the shorthand notation $\Gamma(\tilde{E}_{N+2,N+1}) \equiv \Gamma_{N+2,N+1}$ (we have dropped the tilde for convenience, understanding that all quantities are in dimensionless form). The operator describing the interaction between the SET and oscillator is $\mathcal{V} = \mathcal{V}_1 + \mathcal{V}_2 = \kappa x\mathcal{U}_1 + \epsilon_{\mathrm{HO}}^2\partial/\partial v\mathcal{U}_2$, where

$$\mathcal{U}_1 = \begin{pmatrix} -\Gamma'_{N+2,N+1} & 0 & 0 & 0 & 0 \\ 0 & 0 & \Gamma'_{N+1,N} & 0 & 0 \\ \Gamma'_{N+2,N+1} & 0 & -\Gamma'_{N+1,N} & 0 & 0 \\ 0 & 0 & 0 & -\dfrac{\Gamma'_{N+2,N+1}}{2} & 4\pi r \\ 0 & 0 & 0 & -4\pi r & -\dfrac{\Gamma'_{N+2,N+1}}{2} \end{pmatrix} \tag{10}$$

and

$$\mathcal{U}_2 = \begin{pmatrix} 1+\Delta P & 0 & 0 & 0 & 0 \\ 0 & -1+\Delta P & 0 & 0 & 0 \\ 0 & 0 & \Delta P & 0 & 0 \\ 0 & 0 & 0 & \Delta P & 0 \\ 0 & 0 & 0 & 0 & \Delta P \end{pmatrix}, \tag{11}$$

where we have used the shorthand notation $\Delta P = \langle P_N\rangle - \langle P_{N+2}\rangle$. Note that we have redefined the position coordinate, such that its origin coincides with the steady-state value $\langle x\rangle = -(N+1) + \langle P_N\rangle - \langle P_{N+2}\rangle$, where the steady-state island occupation probabilities are taken to be those for the limit $\kappa \to 0$,

$$\begin{aligned} \langle P_{N+2}\rangle &= \frac{(\pi\epsilon_J)^2}{(\Gamma_{N+2,N+1}/2)^2 + (2\pi r E_{N+2,N})^2 + (\pi\epsilon_J)^2\left(2 + \frac{\Gamma_{N+2,N+1}}{\Gamma_{N+1,N}}\right)}, \\ \langle P_{N+1}\rangle &= \frac{\Gamma_{N+2,N+1}}{\Gamma_{N+1,N}}\langle P_{N+2}\rangle, \\ \langle P_N\rangle &= 1 - \langle P_{N+1}\rangle - \langle P_{N+2}\rangle, \end{aligned} \tag{12}$$

an approach which is valid for sufficiently weak coupling. The advantage of working with this redefined position coordinate will become apparent shortly.

Equation (8) resembles the time-dependent Schrödinger equation. The 'Hamiltonian operator' $\mathcal{H}_0$ gives the free, decoupled evolution of the independent oscillator and SSET systems, while the operator $\mathcal{V} = \mathcal{V}_1 + \mathcal{V}_2$ describes the interaction between the two systems with $\mathcal{V}_1$ giving the dependence of the Cooper-pair and quasi-particle tunnelling rates on the oscillator position and $\mathcal{V}_2$ giving the SSET island number dependence of the electrostatic force acting on the oscillator.

Given the close resemblance of equation (8) to the Schrödinger equation, we can apply approximation techniques developed for open quantum systems, in particular the self-consistent Born approximation (SCBA), followed by the Markov approximation. Applying the SCBA as described in section 3.1 of [27], assuming weak coupling between the oscillator and SSET, $\kappa \ll 1$, we obtain the following approximate expression for the reduced master equation probability distribution $P_{\mathrm{HO}}(x, v, t)$ of the oscillator [10]:

$$\begin{aligned}\dot{P}_{\mathrm{HO}}(x, v, t) = {} & \mathcal{H}_{\mathrm{HO}} P_{\mathrm{HO}}(x, v, t) + \mathrm{e}^{\mathcal{H}_{\mathrm{HO}} t}\mathrm{Tr}_{\mathrm{SET}}[\mathcal{V}(t)\mathcal{P}_{\mathrm{SET}}(0)]\mathrm{e}^{-\mathcal{H}_{\mathrm{HO}} t} P_{\mathrm{HO}}(x, v, t) \\ & - \int_0^t \mathrm{d}t'\, \mathrm{e}^{\mathcal{H}_{\mathrm{HO}} t}\mathrm{Tr}_{\mathrm{SET}}[\mathcal{V}(t)\mathcal{P}_{\mathrm{SET}}(0)]\mathrm{Tr}_{\mathrm{SET}}[\mathcal{V}(t')\mathcal{P}_{\mathrm{SET}}(0)]\mathrm{e}^{-\mathcal{H}_{\mathrm{HO}} t} P_{\mathrm{HO}}(x, v, t) \\ & + \int_0^t \mathrm{d}t'\, \mathrm{e}^{\mathcal{H}_{\mathrm{HO}} t}\mathrm{Tr}_{\mathrm{SET}}[\mathcal{V}(t)\mathcal{V}(t')\mathcal{P}_{\mathrm{SET}}(0)]\mathrm{e}^{-\mathcal{H}_{\mathrm{HO}} t} P_{\mathrm{HO}}(x, v, t), \end{aligned} \tag{13}$$

where $\mathcal{H}_{\mathrm{HO}} = \epsilon^2 x\frac{\partial}{\partial v} - v\frac{\partial}{\partial x}$ is the Hamiltonian operator for the free harmonic oscillator and $\mathcal{V}(t) = \mathrm{e}^{-\mathcal{H}_0 t}\mathcal{V}\mathrm{e}^{+\mathcal{H}_0 t}$ is in the interaction picture. The initial, $t = 0$ probability distribution is taken to be a product state: $\mathcal{P}(0) = P_{\mathrm{HO}}(x, v, 0)\mathcal{P}_{\mathrm{SET}}(0)$, where

$$\mathcal{P}_{\mathrm{SET}}(0) = \begin{pmatrix} P_{N+2}(0) \\ P_N(0) \\ P_{N+1}(0) \\ \mathrm{Im}\, P_{N,N+2}(0) \\ \mathrm{Re}\, P_{N,N+2}(0) \end{pmatrix}.$$

Note that the above SCBA step which gives the oscillator master equation (13) and also the Markov approximation applied below should not be confused with the Born–Markov approximation described earlier in section 2, which gives the starting oscillator–SSET master equation (1); these two approximation steps rely on distinct weak coupling and timescale conditions.

The SCBA approach was applied to obtain a Fokker–Planck equation for a resonator coupled to a normal state SET in [10] and our derivation for the SSET case follows the same route. We can use a Markov approximation and evaluate the integrals in (13) for $t \to \infty$, since typically $\epsilon_{\mathrm{HO}} \ll 1$ and we are only interested in the oscillator dynamics on timescales of the order of the mechanical period and longer, $t \gtrsim \epsilon_{\mathrm{HO}}^{-1}$. Furthermore, using the redefined position coordinate, we find that the second and third terms on the right-hand-side of equation (13) drop out and we eventually obtain

$$\frac{\partial P_{\mathrm{HO}}}{\partial t} = \left[\epsilon_{\mathrm{HO}}^2 x\frac{\partial}{\partial v} - v\frac{\partial}{\partial x} + \kappa\epsilon_{\mathrm{HO}}^2\frac{\partial}{\partial v}(\mathcal{C}_1^{21}x - \mathcal{C}_2^{21}v) + \epsilon_{\mathrm{HO}}^4\frac{\partial}{\partial v}\left(\mathcal{C}_1^{22}\frac{\partial}{\partial v} + \mathcal{C}_2^{22}\frac{\partial}{\partial x}\right)\right] P_{\mathrm{HO}}, \tag{14}$$

where the $\mathcal{C}$ coefficients are defined as follows:

$$\mathcal{C}_1^{ij} = \lim_{t\to\infty} \int_0^t \mathrm{d}\tau\, \mathrm{Tr}[\mathcal{U}_i(t)\mathcal{U}_j(t-\tau)\mathcal{P}_{\mathrm{SET}}(0)] \tag{15}$$

and

$$\mathcal{C}_2^{ij} = \lim_{t\to\infty} \int_0^t \mathrm{d}\tau\, \tau \mathrm{Tr}[\mathcal{U}_i(t)\mathcal{U}_j(t-\tau)\mathcal{P}_{\mathrm{SET}}(0)]. \tag{16}$$

In the Markovian limit, which we have used, these coefficients do not depend on the initial state $\mathcal{P}_{\mathrm{SET}}(0)$ of the SET, just as we would expect. Furthermore, the $\partial^2 P/\partial v\,\partial x$ term in equation (14) (called the 'anomalous diffusion' term in [27]) is of the order of ϵ_{HO} smaller than the diffusion term, when time is expressed in units of the oscillator period; it should have only a small effect on timescales of the order of mechanical period or longer. Re-expressing equation (14) in terms of dimensionful coordinates and dropping the anomalous diffusion term, we obtain

$$\frac{\partial P_{\mathrm{HO}}}{\partial t} = \left(\omega_R^2 x\frac{\partial}{\partial v} - v\frac{\partial}{\partial x} + \gamma_{\mathrm{SET}}\frac{\partial}{\partial v}v + \frac{\gamma_{\mathrm{SET}}k_{\mathrm{B}}T_{\mathrm{SET}}}{m}\frac{\partial^2}{\partial v^2}\right) P_{\mathrm{HO}}, \tag{17}$$

where the renormalized oscillator frequency is

$$\omega_R = \sqrt{1+\kappa\mathcal{C}_1^{21}}\,\omega, \tag{18}$$

the damping rate is

$$\gamma_{\mathrm{SET}} = -\kappa\epsilon_{\mathrm{HO}}\omega\mathcal{C}_2^{21}, \tag{19}$$

and the effective SET temperature is

$$k_{\mathrm{B}}T_{\mathrm{SET}} = -eV_{ds}\frac{\mathcal{C}_1^{22}}{\mathcal{C}_2^{21}}. \tag{20}$$

Equation (17), which has the form of a particular class of Fokker–Planck equation known as the Klein–Kramers equation [28], describes the Brownian motion of a harmonic oscillator interacting with a thermal bath. The oscillator experiences a net damping force, due to the interaction with the SSET (the third term on the right-hand side of equation (17)), and an accompanying Gaussian distributed thermal fluctuating force (the fourth term on the right-hand side of (17), called the 'diffusion' term).

Note that our derivation of the Fokker–Planck equation (17) for the oscillator does not in fact depend on the specifics of the SET interacting with it. As long as the original master equation has the form $\dot{\mathcal{P}} = (\mathcal{H}_0 + \mathcal{V})\mathcal{P}$ with $\mathcal{V} = \mathcal{V}_1 + \mathcal{V}_2 = \kappa x\mathcal{U}_1 + \epsilon_{\mathrm{HO}}^2\frac{\partial}{\partial v}\mathcal{U}_2$, where operators $\mathcal{U}_{1(2)}$ involve only the SET parameters, it then results in the same effective thermal bath description (14) of the SET. The specifics of the SET enter in the dimensionless $\mathcal{C}$ coefficients defined in equations (15) and (16). Thus, for the example of a normal state SET with island electron number fluctuating between the values N and $N+1$, the coefficients take the values $\mathcal{C}_1^{21} = \mathcal{C}_2^{21} = -1$ and $\mathcal{C}_1^{22} = \langle P_N\rangle\langle P_{N+1}\rangle$ [8, 10]. Furthermore, the same approach can be applied to extract the relevant resonator dynamics for the DJQP cycle (see section 3.3 and the appendix).

3. Results

The coefficients $\mathcal{C}_1^{ij}$ and $\mathcal{C}_2^{ij}$, given by equations (15) and (16), together with the Fokker–Planck equation (14), describe the dynamics of a resonator coupled to an SSET. In this section we evaluate equations (15) and (16) numerically to obtain the effective temperature, renormalized frequency and damping of the resonator close to the JQP and DJQP resonances. In order to get a better picture of the underlying physics, and also to understand the limitations of the SCBA approach, we compare these numerical results for the JQP resonance with analytical approximations and numerical results obtained by direct integration of the master equations (given by equation (5)).

We begin this section by presenting approximate analytical results derived for the JQP resonance, as they provide a useful framework within which to understand the resonator dynamics. We then present our numerical results for the JQP and DJQP resonances.

3.1. Analytical approximations for the JQP resonance

It is possible to derive analytical approximations to the $\mathcal{C}$ coefficients as series expansions in ϵ_J. Neglecting also the Γ' terms in the interaction operator $\mathcal{U}_1$, since they are an order of magnitude smaller than the $4\pi r$ terms in $\mathcal{U}_1$, we find the leading non-vanishing order in ϵ_J:

$$\mathcal{C}_1^{21} = -\frac{(4\pi^2 r\epsilon_J)^2 E_{N+2,N}(\Gamma_{N+2,N+1} + 2\Gamma_{N+1,N})}{\Gamma_{N+1,N}[(\Gamma_{N+2,N+1}/2)^2 + (2\pi r E_{N+2,N})^2]^2}, \tag{21}$$

$$\begin{aligned}\mathcal{C}_2^{21} = & -\frac{(4\pi^2 r\epsilon_J)^2 E_{N+2,N}\Gamma_{N+2,N+1}}{\Gamma_{N+1,N}^2[(\Gamma_{N+2,N+1}/2)^2 + (2\pi r E_{N+2,N})^2]^3} \\ & \times [2\Gamma_{N+1,N}^2 + (\Gamma_{N+2,N+1}/2)^2 + \Gamma_{N+1,N}\Gamma_{N+2,N+1} + (2\pi r E_{N+2,N})^2],\end{aligned} \tag{22}$$

$$\begin{aligned}\mathcal{C}_1^{22} = & \frac{(\pi\epsilon_J)^2\Gamma_{N+2,N+1}}{\Gamma_{N+1,N}^2[(\Gamma_{N+2,N+1}/2)^2 + (2\pi r E_{N+2,N})^2]^2} \\ & \times [2\Gamma_{N+1,N}^2 + (\Gamma_{N+2,N+1}/2)^2 + \Gamma_{N+1,N}\Gamma_{N+2,N+1} + (2\pi r E_{N+2,N})^2].\end{aligned} \tag{23}$$

The approximations to the renormalized frequency, damping rate and effective SET temperature then follow by substituting (21), (22) and (23) into equations (18), (19) and (20). In particular, for the SET temperature, we have:

$$k_B T_{\mathrm{SET}} = -eV_{ds}\frac{\mathcal{C}_1^{22}}{\mathcal{C}_2^{21}} = \frac{\hbar}{4}\frac{\Gamma_{N+2,N+1}^2 + 4(E_{N+2,N}/\hbar)^2}{4(E_{N+2,N}/\hbar)}, \tag{24}$$

where $\Gamma_{N+2,N+1}$ and $E_{N+2,N}$ are in their original, dimensional form (see equations (2) and (4)). Note that T_{SET} does not depend on ϵ_J to leading order, while γ_{SET} and the frequency renormalization are $O(\epsilon_J^2)$.

Although these results are simple and intuitive, they are in principle only valid when $\pi\epsilon_J \ll 1$, a condition which is by no means always satisfied for SSETs in practice.

3.2. Numerical results for the JQP resonance

Two distinct sets of numerical calculations are carried out. We carry out integrations of the original master equations and within the framework of the Born–Markov approximation (5), we evaluate the expressions for the coefficients (equations (15) and (16)) numerically.

For the numerical integration of the master equations [8], we obtain the full evolution of the resonator probability distribution (with initial state chosen to be Gaussian) from which we determine the evolution of the average position (with respect to the fixed point value), $\langle x(t)\rangle$. We then obtain values for ω_R and $\gamma_{\rm SET}$ by fitting $\langle x(t)\rangle$ to the equation of motion of a damped harmonic oscillator with a renormalized frequency. Finally, we use equations (18) and (19) to infer values of the corresponding coefficients. In obtaining these results, we concentrate on the typical experimentally accessible regime $\kappa, \epsilon \ll 1$. As a consequence, the numerical integrations take a prohibitively long time to reach a steady state and so we do not extract values of $T_{\rm SET}$ from the integrations.

Figures 3 and 4 show our numerical calculations of the coefficients $\mathcal{C}_1^{21}, \mathcal{C}_2^{21}$ and $T_{\rm SET}$, with the corresponding analytical approximations (21), (22) and (24) shown for comparison. Notice that while the numerical results for $\mathcal{C}_1^{21}$ and $\mathcal{C}_2^{21}$ were obtained from numerical integrations of both the master equations (without Born–Markov approximation) and from equations (15) and (16) (with the Born–Markov approximation), the numerical results for $T_{\rm SET}$ were only obtained using the latter technique. In the numerics, values for the system parameters were chosen that are typical of those found in current devices [5, 6]. In particular, the value of $\epsilon_J = \Delta/(8eV_{ds}) = 1/16$ is kept relatively small. This value corresponds to choosing $eV_{ds} = 2\Delta$, the correct order of magnitude to enable the JQP and DJQP cycles. Nevertheless, it is clear from figure 3 that our analytical approximations differ substantially from the numerics in the vicinity of the resonance. In contrast, figure 4 shows that there is excellent agreement between the analytical and numerical calculations of $T_{\rm SET}$. It is not clear why the agreement is so good, but the most obvious explanation is that the cancellation of the ϵ_J-dependent terms that occurs in our approximate expression for the ratio $\mathcal{C}_1^{22}/\mathcal{C}_2^{21}$ must extend beyond second order in ϵ_J.

Figure 5 shows schematically the V_{ds} and V_g bias ranges in relation to the JQP resonance lines for which the curves in figures 3 and 4 are obtained. Note that, because the quasi-particle tunnel rates and their gradients have been approximated as constants equal to unity for simplicity, the JQP curves in figures 3 and 4 do not depend on the V_{ds} bias choice. With the dependences of the tunnel rates on the energies $E_{N+2,N+1}$ and $E_{N+1,N}$ properly taken into account (see equations (2) and (3)), one finds that the maximum and minimum values of the $\mathcal{C}_1^{21}$ and $\mathcal{C}_2^{21}$ curves increase in magnitude as V_{ds} decreases towards the onset for the JQP cycle at $eV_{ds} = 2\Delta + E_c$. In contrast, as we shall see below, the DJQP curves depend strongly on the V_{ds} bias choice even when the quasi-particle tunnel rates are approximated as constants.

The results obtained from the numerical integrations of the master equations agree well with those obtained within the Born–Markov approximation. As expected, the agreement between the two improves as the magnitude of κ is reduced, in accord with our use of the approximation $\kappa \ll 1$ in deriving the reduced master equation.

In addition, the numerical integration of the master equations gives us one more piece of information that we could not have obtained from our calculations within the Born–Markov approximation. Very close to the resonance, we find that the evolution of $\langle x(t)\rangle$ no longer matches

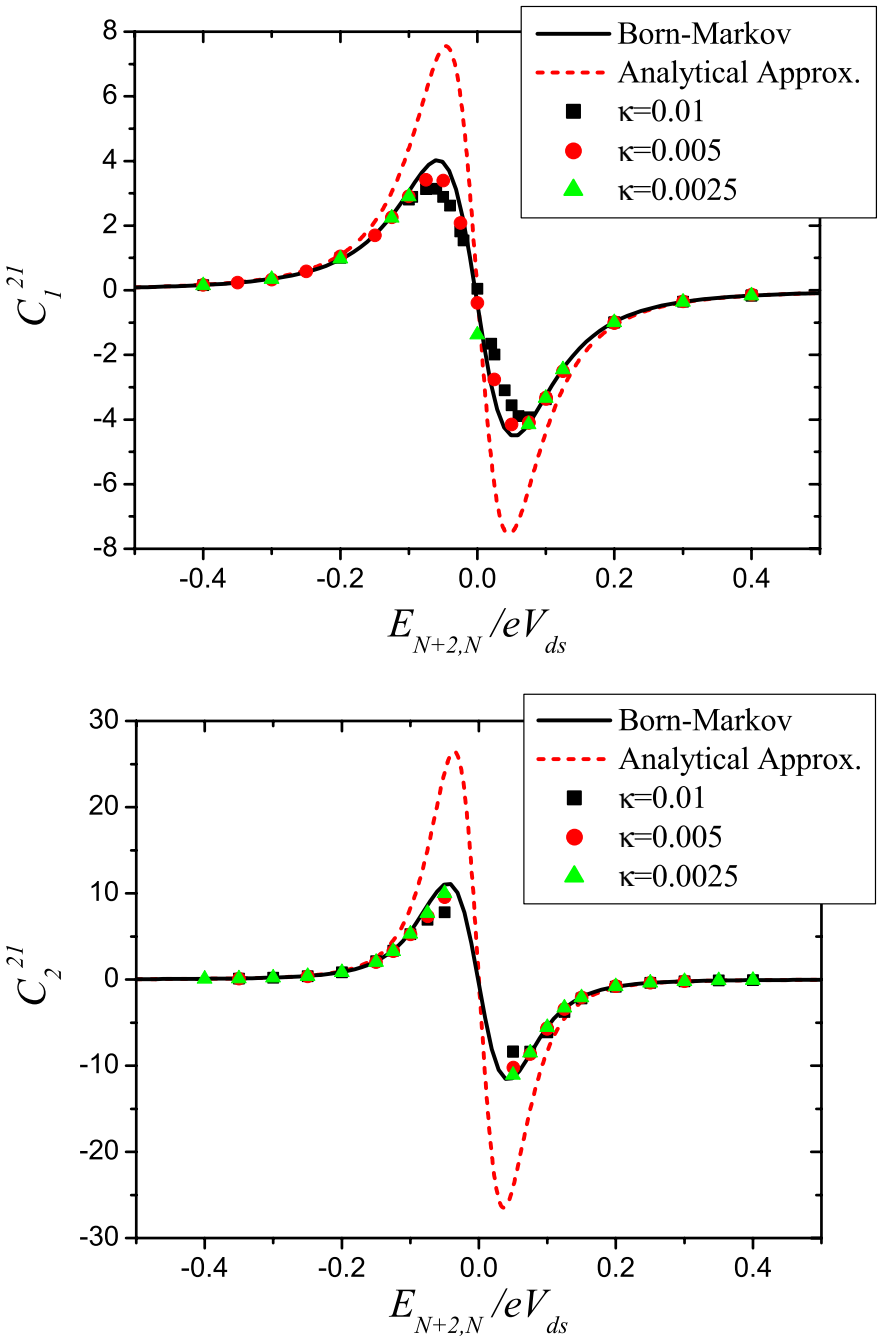

Figure 3. Comparison of numerical calculations of the coefficients $\mathcal{C}_1^{21}$ and $\mathcal{C}_2^{21}$ with the analytical approximations (equations (21) and (22)). The full curves come from numerical evaluations of equations (15) and (16), whereas the points come from numerical integrations of the master equations (5). For the numerics, we choose $\epsilon_J = 1/16, r = 1$ and set the quasi-particle tunnel rates and their gradients to unity. In addition, when integrating the master equations we set $\epsilon = 0.1$ and vary the value of κ as shown.

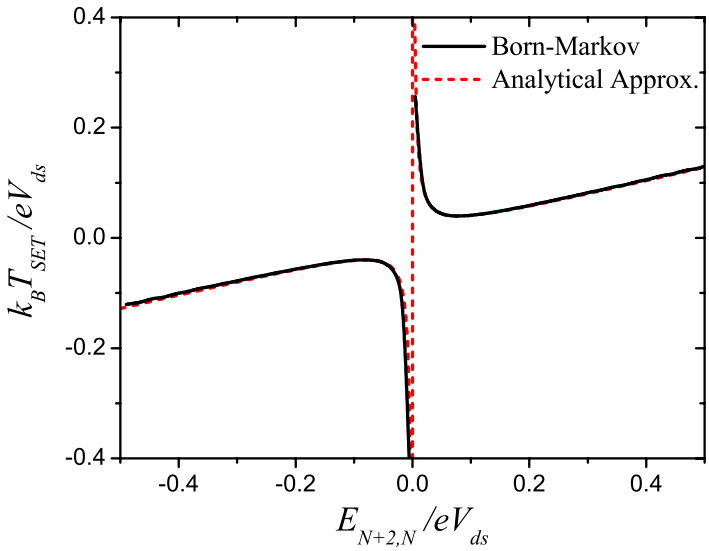

Figure 4. Comparison of numerical calculations of T_{SET} with the analytical approximation, equation (24). The parameters are the same as those used for figure 3.

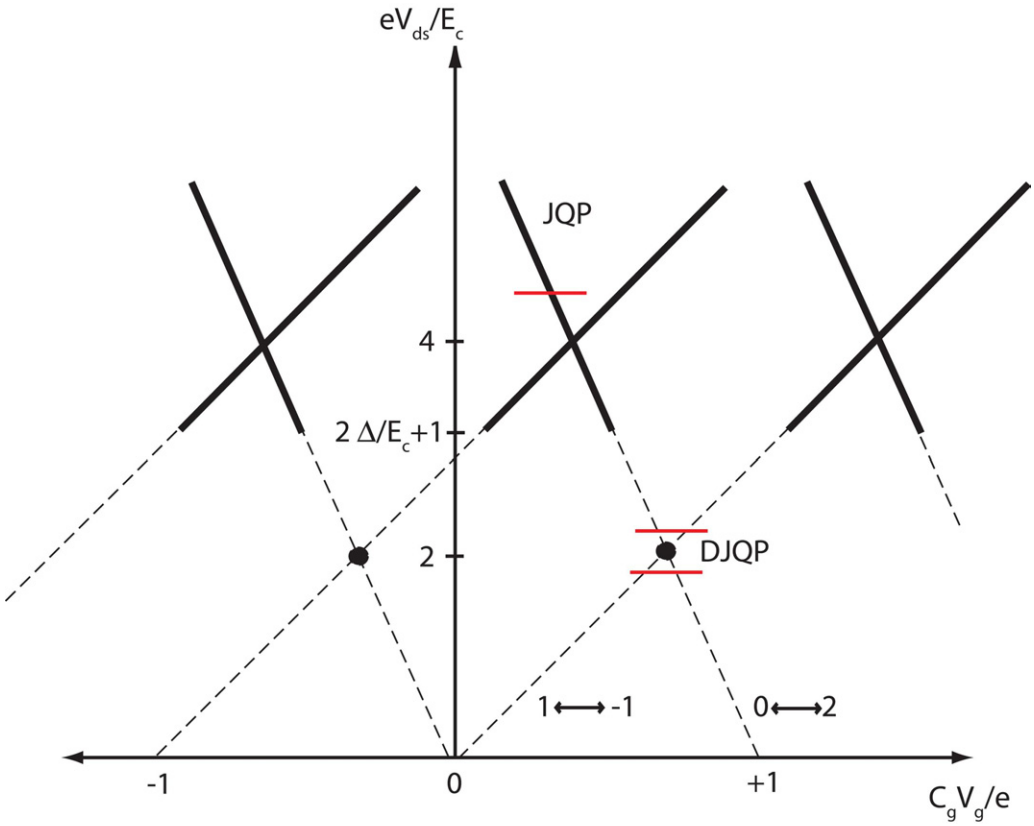

Figure 5. Schematic map showing the location of a selection of neighbouring JQP resonances (solid black lines) and DJQP resonances (solid black circles). The bias ranges for the $\mathcal{C}_1^{21}$, $\mathcal{C}_2^{21}$ and T_{SET} plots are indicated by the solid red lines.

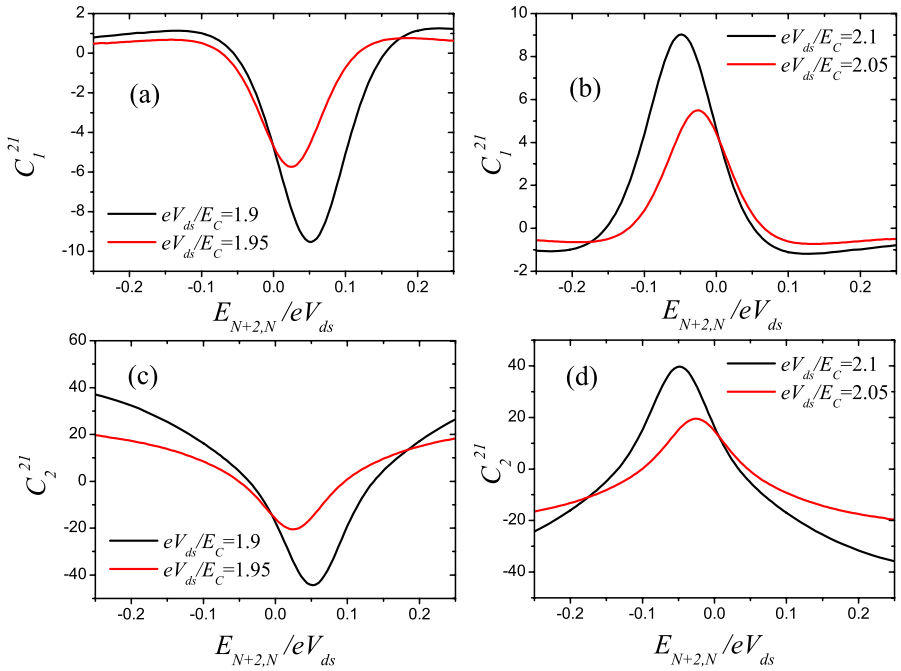

Figure 6. Numerical calculations of the coefficients $\mathcal{C}_1^{21}$ and $\mathcal{C}_2^{21}$ in the vicinity of the DJQP resonance. The different values of E_C/eV_{ds} correspond to points at different distances below, (a) and (c), and above, (b) and (d), the centre of the DJQP resonance (see figure 5). As before, we choose $\epsilon_J = 1/16$, $r = 1$ and set the quasi-particle tunnel rates and their gradients to unity.

that of a damped harmonic oscillator.[5] Thus, it seems that very close to the resonance the action of the SSET on the resonator is not analogous to a thermal bath. Although we have not carried out a systematic investigation of the region in which deviations from thermal bath-like behaviour occur, we do find that the width of the region (in terms of $E_{N+2,N}$) broadens with increasing κ. This suggests that the weak coupling (Born) approximation we use to derive the Fokker–Planck equation may break down for $m\omega_0^2 x_s^2 \gtrsim E_{N+2,N}$ (i.e. $\kappa \gtrsim \tilde{E}_{N+2,N}$).

3.3. DJQP resonance

The coefficients $\mathcal{C}_1^{21}$ and $\mathcal{C}_2^{21}$ calculated within the Born–Markov approximation are shown in figure 6, while the corresponding variation in T_{SET} is shown in figure 7. To facilitate comparisons with the JQP resonance, we have chosen $\tilde{E}_{N+2,N}$ and eV_{ds}/E_c as independent variables, in terms of which the detuning of other energies is given by $\tilde{E}_{N+1,N-1} = \tilde{E}_{N+2,N} - 4(E_c/eV_{ds}) + 2$. The relation between the range of SET bias points covered in figures 6 and 7 are illustrated schematically in figure 5.

[5] The points plotted in figure 3 were all obtained from a fit to the behaviour of a damped harmonic oscillator. Close to the resonance, where this fit is not readily obtained we were not able to extract values for $\gamma_{\rm SET}$ and hence no corresponding data points are plotted for $\mathcal{C}_2^{21}$.

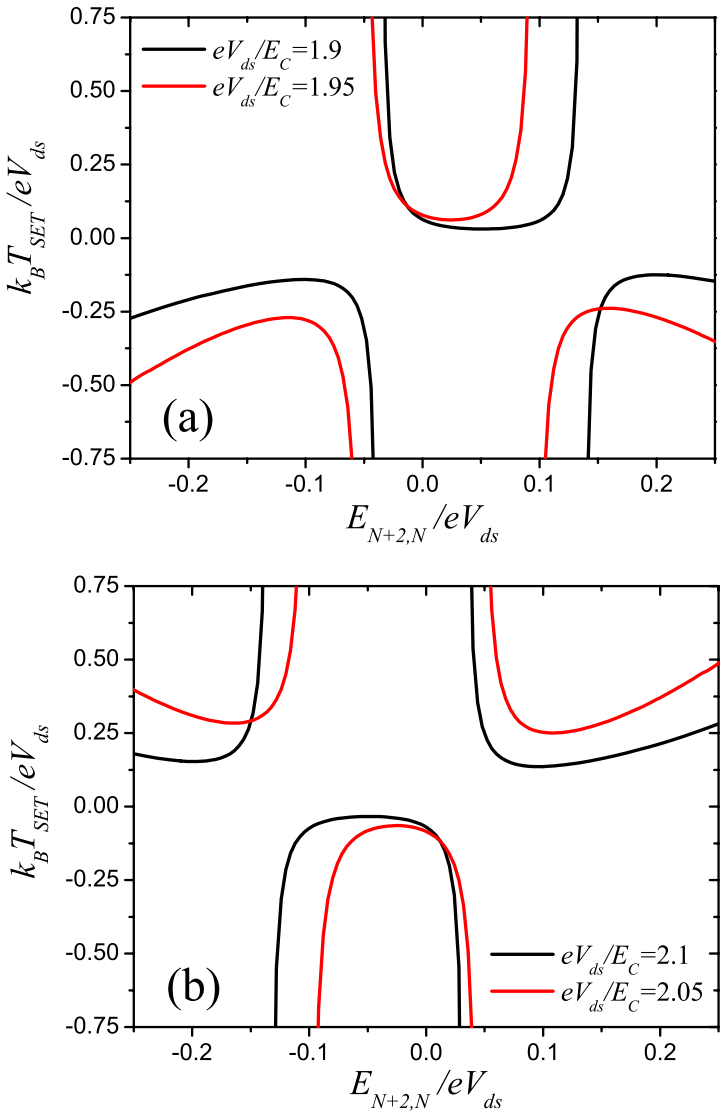

Figure 7. Numerical calculation of T_{SET} (a) below and (b) above the DJQP resonance. The parameters are the same as those used for figure 6.

The DJQP resonance is much more complex than the JQP one and our results by no means cover the whole range of the relevant parameter space. However, by comparing figures 3 and 6, it is clear that the magnitude of $\mathcal{C}_2^{21}$, and hence γ_{SET}, is generally much larger for the DJQP resonance than for the JQP one. As we shall discuss below, this implies that in an experiment the effects of the back-action due to the SSET on the resonator dynamics will be stronger when close to the DJQP resonance.

By analogy with the JQP resonance, it seems inevitable that there will be regions very close to the DJQP resonances, where our Born–Markov approximation will fail to capture fully the physics of the system. However, because of the additional complexity of the DJQP cycle, we have not as yet performed the necessary numerical integrations of the master equations required to determine exactly where and how the Born–Markov approach breaks down.

4. Discussion and conclusions

We now turn to consider the implications of our results for experiments on nanomechanical–SET systems and to explore the analogies which exist with other physical systems.

In an experiment, the overall state of the resonator would be determined by the combined effects of the SSET and the external surroundings of the resonator other than the SSET, which can be modelled by a damping rate, γ_e, and a temperature, T_e. The overall effective temperature and damping rate of the resonator would be given by the weighted averages [8],

$$\gamma_{\rm eff} T_{\rm eff} = \gamma_{\rm SET} T_{\rm SET} + \gamma_e T_e, \tag{25}$$

$$\gamma_{\rm eff} = \gamma_{\rm SET} + \gamma_e. \tag{26}$$

From these relations, it is clear that when $\gamma_{\rm SET}$ becomes negative $\gamma_{\rm eff}$ will decrease, eventually leading to a dynamic instability in the state of the resonator, when $\gamma_{\rm eff} \leqslant 0$. However, we should point out that the model described here is not sufficiently robust to explore precisely what would happen in this regime.

The expressions for the effective temperature and damping rate also make clear that for $\gamma_{\rm SET} \gg \gamma_e$, the effective temperature of the resonator will be dominated by $T_{\rm SET}$. This has a number of important implications given the minima in $T_{\rm SET}$, which develop close to the JQP and DJQP resonances. For example, the minimum value of $T_{\rm SET}$ which is simply proportional to the quasi-particle decay rate can easily be as low as $\sim$100 mK, suggesting that the electronic back-action on the resonator could be demonstrated in a dramatic way by using the SSET to cool the resonator when $T_e > T_{\rm SET}$. Indeed a close analogy can be made between the temperature of a resonator coupled to an SSET and that of (two-level) atoms undergoing Doppler cooling due to counter-propagating laser beams [22, 23].

In Doppler cooling, the interaction between laser beams and two of the atoms' energy levels leads to an effective damping of the atomic translational motion. The atoms are cooled to a temperature that depends on the detuning of the laser light from the atomic resonance,[6] Δ, and the decay rate of the excited atomic state, Γ_e, given by the relation [23]

$$k_{\rm B} T_{\rm Doppler} = \frac{\hbar}{4} \frac{\Gamma_e^2 + 4\Delta^2}{2\Delta}. \tag{27}$$

This equation has an almost identical form to that for $T_{\rm SET}$ close to the JQP resonance (equation (24)). It is interesting to note that a more direct analogy between Doppler cooling and a system consisting of a resonator coupled to a Cooper pair box [29] addressed by an additional, fixed voltage gate was suggested recently [30]. The effective temperature of the resonator in that case takes exactly the same form as that near the JQP resonance when an appropriate ac-voltage is applied to the extra fixed gate [30], although the relevant decay rate is not related to quasi-particle tunnelling and the associated expression for the damping of the resonator takes a different form to that considered here.

Another system that might be expected to have very similar dynamics to the SSET-resonator system is that of a double quantum dot (DQD) gated by a mechanical resonator [31]. Since DQDs

[6] Note we define the detuning, Δ, with the opposite sign to that given in [23].

display an electronic resonance which is in many ways analogous to the JQP cycle, the dynamics of a resonator coupled to a DQD should be very similar to that of one coupled to an SSET near the JQP resonance. Experiments on DQD-resonator systems have not yet been performed, but work on gating individual quantum dots by mechanical resonators [32] demonstrates that such systems are certainly a feasible prospect.

Our work raises a number of interesting questions for future research. For example, in the regime that we examined, the strongly nonlinear properties of the quasi-particle-tunnelling rates played no role. It would be interesting to examine the dynamics of the resonator for parameters close to the threshold for quasi-particle tunnelling, so that the motion of the resonator itself could control whether or not tunnelling occurs. Also of interest is our finding that the self-consistent Born–Markov approximation method apparently cannot capture the physics of the system when it is tuned extremely close to the JQP resonance; this raises the intriguing possibility that the resonator dynamics in this regime differs substantially from the thermalized dynamics described here. Furthermore, we have not yet examined the conditions under which the Born–Markov approximation breaks down for the DJQP resonance, although this is an area we plan to explore in future work.

In conclusion, we have found that, like a normal state SET, an SSET in the vicinity of either the JQP or DJQP resonance acts on a nanomechanical resonator like an equilibrium thermal bath for sufficiently weak electro-mechanical coupling and for sufficiently large separation between the electrical and mechanical timescales. However, the effective temperature, damping and frequency shift of the resonator due to an SSET close to the JQP and DJQP resonances take very different forms, both from each other and from the normal state SET. In particular, the magnitude and even the sign of the effective temperature and damping for the SSET depend very sensitively on where it is tuned with respect to either the JQP or DJQP resonance.

Acknowledgments

We gratefully acknowledge a number of very fruitful discussions with O Buu, M D LaHaye, A J Rimberg, K C Schwab and especially A A Clerk. MPB would also like to thank S Tamura and the University of Hokkaido for their hospitality where some of this work was carried out, as well as the support of a Japan Society for the Promotion of Science Fellowship. MPB acknowledges funding from the NSF under NIRT grant CMS-0404031. JI and ADA acknowledge support from the EPSRC under grant GR/S42415/01.

Appendix. Master equations for the DJQP resonance

In this appendix, we present the semiclassical master equations for the SSET-resonator system in the vicinity of the DJQP resonance. As shown schematically in figure 2(b), the DJQP cycle [19, 20, 33] involves resonant Cooper-pair tunnelling at each junction alternating in turn with two quasi-particle tunnelling events.

The semiclassical master equations for the SSET resonator near the DJQP resonance are derived using the same procedure as for the JQP resonance. In dimensionless notation, they take

the form [33],

$$\dot{\rho}_{N-1} = \epsilon_{\mathrm{HO}}^2[x + (N-1)]\frac{\partial \rho_{N-1}}{\partial v} - v\frac{\partial \rho_{N-1}}{\partial x} + \mathrm{i}\pi\epsilon_J(\rho_{N+1,N-1} - \rho_{N-1,N+1}) - [\tilde{\Gamma}(\tilde{E}_{N-1,N}) + \tilde{\Gamma}'(\tilde{E}_{N-1,N})\kappa x]\,\rho_{N-1}, \tag{A.1}$$

$$\dot{\rho}_{N} = \epsilon_{\mathrm{HO}}^2(x + N)\frac{\partial \rho_{N}}{\partial v} - v\frac{\partial \rho_{N}}{\partial x} + \mathrm{i}\pi\epsilon_J(\rho_{N+2,N} - \rho_{N,N+2}) + [\tilde{\Gamma}(\tilde{E}_{N-1,N}) + \tilde{\Gamma}'(\tilde{E}_{N-1,N})\kappa x]\,\rho_{N-1}, \tag{A.2}$$

$$\dot{\rho}_{N+1} = \epsilon_{\mathrm{HO}}^2[x + (N+1)]\frac{\partial \rho_{N+1}}{\partial v} - v\frac{\partial \rho_{N+1}}{\partial x} - \mathrm{i}\pi\epsilon_J(\rho_{N+1,N-1} - \rho_{N-1,N+1}) + [\tilde{\Gamma}(\tilde{E}_{N+2,N+1}) + \tilde{\Gamma}'(\tilde{E}_{N+2,N+1})\kappa x]\,\rho_{N+2}, \tag{A.3}$$

$$\dot{\rho}_{N+2} = \epsilon_{\mathrm{HO}}^2[x + (N+2)]\frac{\partial \rho_{N+2}}{\partial v} - v\frac{\partial \rho_{N+2}}{\partial x} - \mathrm{i}\pi\epsilon_J(\rho_{N+2,N} - \rho_{N,N+2}) - [\tilde{\Gamma}(\tilde{E}_{N+2,N+1}) + \tilde{\Gamma}'(\tilde{E}_{N+2,N+1})\kappa x]\,\rho_{N+2}, \tag{A.4}$$

$$\dot{\rho}_{N-1,N+1} = \epsilon_{\mathrm{HO}}^2(x + N)\frac{\partial \rho_{N-1,N+1}}{\partial v} - v\frac{\partial \rho_{N-1,N+1}}{\partial x} + \mathrm{i}\pi\epsilon_J(\rho_{N+1} - \rho_{N-1}) + [2\pi\mathrm{i}r(\tilde{E}_{N+1,N-1} + 2\kappa x) - \tfrac{1}{2}(\tilde{\Gamma}(\tilde{E}_{N-1,N}) + \tilde{\Gamma}'(\tilde{E}_{N-1,N})\kappa x)]\,\rho_{N-1,N+1}, \tag{A.5}$$

$$\dot{\rho}_{N,N+2} = \epsilon_{\mathrm{HO}}^2[x + (N+1)]\frac{\partial \rho_{N,N+2}}{\partial v} - v\frac{\partial \rho_{N,N+2}}{\partial x} + \mathrm{i}\pi\epsilon_J(\rho_{N+2} - \rho_{N}) + [2\pi\mathrm{i}r(\tilde{E}_{N+2,N} + 2\kappa x) - \tfrac{1}{2}(\tilde{\Gamma}(\tilde{E}_{N+2,N+1}) + \tilde{\Gamma}'(\tilde{E}_{N+2,N+1})\kappa x)]\,\rho_{N,N+2}. \tag{A.6}$$

The relevant energy differences for the quasi-particle and Cooper-pair tunnelling processes involved in the DJQP cycle are given by

$$E_{N+2,N+1} = -2E_c(N_g - N - 3/2) + eV_{ds}, \tag{A.7}$$

$$E_{N-1,N} = 2E_c(N_g - N + 1/2), \tag{A.8}$$

and

$$E_{N+2,N} = -4E_c(N_g - N - 1), \tag{A.9}$$

$$E_{N+1,N-1} = -4E_c(N_g - N) + 2eV_{ds}, \tag{A.10}$$

respectively. The DJQP resonance occurs when $E_{N+2,N} = E_{N-1,N+1} = 0$, i.e. when $eV_{ds} = 2E_c$ and $N_g = N + 1$. Notice that the cycle also requires that the quasi-particle-tunnelling processes are not energetically forbidden, which implies that $E_c > 2\Delta/3$, if we assume for simplicity that the superconductors are at zero temperature.

These master equations give rise to a Fokker–Planck equation with the same form as equation (14), but with different expressions for the coefficients $\mathcal{C}_1^{21}$, $\mathcal{C}_2^{21}$, $\mathcal{C}_1^{22}$ and $\mathcal{C}_2^{22}$. These coefficients can be calculated numerically, in the same way as those for the JQP resonance, to give the results presented in section 3.3.

References

[1] White J D 1993 *Japan. J. Appl. Phys. Part 2* **32** L1571
[2] Blencowe M P and Wybourne M N 2000 *Appl. Phys. Lett.* **77** 3845
[3] Zhang Y and Blencowe M P 2002 *J. Appl. Phys.* **91** 4249
[4] Blencowe M P 2004 *Phys. Rep.* **395** 159
[5] Knobel R S and Cleland A N 2003 *Nature* **424** 291
[6] LaHaye M D, Buu O, Camarota B and Schwab K C 2004 *Science* **304** 74
[7] Mozyrsky D, Martin I and Hastings M B 2004 *Phys. Rev. Lett.* **92** 018303
[8] Armour A D, Blencowe M P and Zhang Y 2004 *Phys. Rev.* B **69** 125313
[9] Armour A D 2004 *Phys. Rev.* B **70** 165315
[10] Blencowe M P 2005 *Contemp. Phys.* **46** 249
[11] Mozyrsky D and Martin I 2002 *Phys. Rev. Lett.* **89** 018301
[12] Clerk A A and Girvin S M 2004 *Phys. Rev.* B **70** 121303
[13] Clerk A A 2004 *Phys. Rev.* B **70** 245306
[14] Schoeller H and Schön G 1994 *Phys. Rev.* B **50** 18436
[15] Averin D V and Aleshkin V Ya 1989 *Sov. Phys.—JETP Lett.* **50** 367
[16] Nakamura Y, Chen C D and Tsai J S 1996 *Phys. Rev.* B **53** 8234
[17] Fitzgerald R J, Pohlen S L and Tinkham M 1998 *Phys. Rev.* B **57** R11073
[18] Choi M S, Fazio R, Siewert J and Bruder C 2001 *Europhys. Lett.* **53** 251
Choi M S, Plastina F and Fazio R 2003 *Phys. Rev.* B **67** 045105
[19] Clerk A A, Girvin S M, Nguyen A K and Stone A D 2002 *Phys. Rev. Lett.* **89** 176804
[20] Thalakulam M, Ji Z and Rimberg A J 2004 *Phys. Rev. Lett.* **93** 066804
[21] Clerk A A and Bennett S 2005 *New J. Phys.* **7** 238
[22] Stenholm S 1986 *Rev. Mod. Phys.* **58** 699
[23] Lett P D, Phillips W D, Rolston S L, Tanner C E, Watts R N and Westbrook C I 1989 *J. Opt. Soc. Am.* B **6** 2084
[24] Agarwal G S 1969 *Phys. Rev.* **178** 2025
[25] Martens C C and Fang J-Y 1997 *J. Chem. Phys.* **106** 4918
[26] Nakamura Y, Korotkov A N, Chen C D and Tsai J S 1997 *Phys. Rev.* B **56** 5116
[27] Paz J P and Zurek W H 2000 *Coherent Atomic Matter Waves: Les Houches-Ecole d'Été de Physique Théorique* vol 72, ed R Kaiser, C Westbrook and F David (Berlin: Springer) (*Preprint* quant-ph/0010011)
[28] Risken H 1989 *The Fokker–Planck Equation* (Berlin: Springer)
[29] Armour A D, Blencowe M P and Schwab K C 2002 *Phys. Rev. Lett.* **88** 148301
[30] Martin I, Shnirman A, Tian L and Zoller P 2004 *Phys. Rev.* B **69** 125339
[31] Brandes T and Lambert N 2003 *Phys. Rev.* B **67** 125323
[32] Weig E M, Blick R H, Brandes T, Kirschbaum J, Wegscheider W, Bichler M and Kotthaus J P 2004 *Phys. Rev. Lett.* **92** 046804
[33] Clerk A A 2003 *New Directions in Mesocsopic Physics, NATO ASI* ed R Fazio, V F Gantmakher and Y Imry (Dordrecht: Kluwer) p 325